M E R C A T O R M A S T E R P R O J E C T

APPLICATION FOR GUARANTEED TIME ON MERCATOR

To be submitted to: degenaar@uva.nl, r.a.d.wijnands@uva.nl, e.j.m.koo@uva.nl Year: **2025**

1. Title

Probing Wind Clumping in Wolf-Rayet + O-Star Binary WR 140 in Post-Periastron Period using HERMES Spectroscopy

2. Abstract

Wolf-Rayet (WR) stars lose mass via powerful, radiatively driven winds that are structured and clumpy, and their poorly constrained acceleration zones introduce key uncertainties into stellar-evolution models. The wind-acceleration parameter β determines the velocity profile of the stellar wind. This profile also affects the mass-loss rate. For WR 140, a benchmark WR+O massive binary, β remains unmeasured due to severe spectral contamination near periastron, caused by strong wind-wind shocks and extensive line blending. We will obtain 25 high-resolution ($R \approx 85{,}000$) HERMES spectra during the post-periastron "clean window" ($\phi \approx 0.1$) to track Doppler shifts of wind clumps and recover their accelerations. This will give the first precise measurement of β in this system, eliminate the dominant uncertainty in WR 140's mass-loss rate, and provide a transferable benchmark for calibrating wind and clumping physics in binary massive-star evolution models.

3.

Run	Period	Instrument	Time	Month	Moon	Seeing	Sky Trans.	Obs.Mode
A	25	HERMES	3.3 h	Oct	n	n	CLR	v

4. Special remarks:

Our schedule is flexible: the 3 main nights of intensive monitoring can be arranged on any 3 nights within a 10-day window around $\phi \approx 0.1$, depending on telescope availability.

5. Students:

Anmolsingh Marwaha (Amsterdam, NL), Qianhang Chen (Amsterdam, NL), Haotian Sun (Amsterdam, NL)

6. Description of the proposed programme (max. 2 pages)

A) Scientific Rationale:

Massive stars and the puzzle of mass loss. Mass loss from massive stars profoundly influences their evolution and fate but remains one of the least constrained processes in stellar astrophysics. In Wolf–Rayet (WR) stars, extreme, radiatively driven winds remove significant mass and angular momentum, profoundly altering their evolutionary path. However, these winds are clumped and inhomogeneous, dominated by clumpy substructures formed via the line-driven instability (LDI; Owocki & Rybicki 1984). Such clumping introduces low-level variability in optical lines (Eversberg et al. 1998) and leads to significant uncertainties in derived mass-loss rates, potentially underestimating them by a factor of ~ 2 or more (Oskinova et al. 2007; Sundqvist et al. 2011).

Open questions: The missing wind acceleration parameter β. The wind acceleration parameter β directly impacts derived mass-loss rates, since uncertainties in wind velocity structure propagate into substantial uncertainties in mass-loss determinations. A fundamental parameter characterizing stellar wind dynamics is the acceleration parameter β, describing how quickly the wind accelerates from the stellar surface to its terminal velocity, typically expressed via the β-law,

$$v(r) \propto \left(1 - R/r\right)^{\beta}.$$

WR 140 is one of the few WR+O binaries whose geometry, distance, and component masses are simultaneously fixed by CHARA/IOTA astrometry and double-lined RVs: Monnier et al. (2011) give $d = 1.67 \pm 0.03$ kpc and $M_{\rm WR} = 14.9 \pm 0.5\,M_{\odot}$, parameters that Pollock et al. (2021) describe as "exceptionally well-determined." Previous periastron campaigns on WR 140 ($P \approx 7.9$ yr, $e \approx 0.88$) yielded a superb orbit but failed to isolate the intrinsic β: the He I 1.083 μm "periastron sub-peak" discovered by Fahed et al. (2011) and modeled by Williams et al. (2021) is powered by shock-heated gas whose flux outshines the contemporaneous IR/X-ray burst, and the O5 absorption blends with the WR wind when the stars are closest. Hence, periastron spectra are too contaminated for a β fit, so all X-ray/IR models to date (e.g. Sundqvist et al. 2011) still assume canonical $\beta \approx 1$–3.

Ideal observation time: The true "clean window" opens in post-periastron at $\phi \approx 0.10$, as explained in Figure 1. By then the shock has moved out of the line of sight, line blending is minimal, and the P Cygni absorption in He I λ5876, C III λ5696, C IV λ5808, etc., forms in the unperturbed WC7 wind. Clumps seen at this phase sample velocities 2–3 × higher than at periastron, giving direct leverage on β; they also probe whether clumps truly survive the collision (Gunawan et al. 2001; Dougherty et al. 2005; Lepine & Moffat 1999; Zhekov 2021). We propose to use the high-resolution (R ≈ 85,000) HERMES spectrograph on the Mercator telescope to obtain 25 optical spectra of WR 140 during $\phi \approx 0.10$. We aim for a signal-to-noise ratio of 200 to detect subtle variations in emission and absorption features, subtract average line profiles at each epoch and, following Lefèvre et al. (2005), convert Doppler-shift evolution into radial trajectories to fit an empirical β-law for the first direct measurement in WR 140.

Scientific impact: Clarifying stellar evolution models. This study will deliver the first definitive measurement of β in the well-characterized WR binary WR 140, substantially improving mass-loss prescriptions and wind-acceleration models. Tracking clump survival post-shock will yield new insights into wind clumping dynamics. Our results will inform multi-wavelength simulations of WR wind interactions (X-ray, IR) and provide a template for similar studies in other eccentric massive binaries, ultimately refining stellar-evolution codes and deepening our understanding of mass-loss physics in massive stars. In particular, our measurement of β allows us to derive the local wind speed $V_{\rm flow}$ at the collision region. Combined with the observed line-of-sight velocity V_r which traces material along the surface of the shock cone from infrared shock tracers (Williams et al. 2021), this enables a geometric determination of the shock-cone opening angle θ, and thus a more accurate estimate of the wind-momentum ratio η. Since poor constraints on η are a major source of uncertainty in WR mass-loss rates (Dougherty et al. 2005), our results will help break this degeneracy and provide a more robust determination of $\dot{M}_{\rm WR}$, a key quantity in massive-star evolution.

B) Immediate Objective:

The primary objective of our observations is to constrain the wind-acceleration parameter β of the WR 140 system by tracking the acceleration of individual clumps in the stellar wind. This will be achieved through time-resolved, high-resolution spectral monitoring of prominent emission lines such as CIII 5696, CIV (5471 and 5805), OV 5592, and HeI 5876, whose profile variability encodes information about wind dynamics.
We propose to obtain **25 high-resolution optical spectra** using the HERMES spectrograph in HRF mode on the 1.2-m Mercator Telescope. Our program consists of a three-night intensive monitoring campaign with

six spectra per night, evenly distributed over a five-hour interval to resolve short-term variability. In addition, we will obtain one spectrum per night over seven consecutive nights to constrain the high-velocity end of the β-law fitting and assess clump lifetimes through cross-night comparison of spectral substructures.

C) Technical feasibility and Strategy

Justification of Target: WR 140 is among the few known WR+O systems with a fully solved 3D orbit and parallax distance. Combined interferometric and spectroscopic analyses yield a distance of $d = 1.67 \pm 0.03$ kpc, and component masses of $M_{\rm WR} = 15\,M_\odot$ and $M_{\rm O} = 36\,M_\odot$ (Pollock et al. 2021). Pollock et al. (2021) describe its long-period, highly eccentric orbit as exceptionally well-determined.

Spectra Cleanliness: The optical contribution of the O star companion in WR 140 is restricted to a handful of 1 Å photospheric absorptions, while the broad WC7 wind features remain uncontaminated. In the 5400–5900 Å window that contains our key diagnostics C III 5696 and He I 5876, Marchenko et al. (2003) mark every O-star line with downward arrows and show that they occupy only the line cores, leaving the $\pm$ 400kms^{-1} wings completely clean. Fahed et al. (2011) reached the same conclusion with a shift-and-add decomposition: once the narrow cores are subtracted, the residual profile is "practically unaffected" outside those channels. Together, these studies show that the O-star contribution is negligible, so it can be safely ignored when fitting the -law to the WC7 wind. This is presented in Figure 2.

Justification of the Exposure Time: To detect line-profile variations as small as 0.5%, corresponding to a 1σ detection threshold, a signal-to-noise ratio (S/N) of at least 200 per pixel at 550 nm is required (Lefèvre et al. 2005). WR 140 has a visual magnitude of $V = 6.85$, and based on the performance of the HERMES spectrograph, such S/N levels are achievable in 8 minutes.

Observation Plan: WR 140 is well positioned for observation from La Palma in early October. By 21:00 local time, the sky is fully dark and the target reaches an altitude of 75°, remaining above 30° until 02:00. This provides an uninterrupted ∼5-hour nightly window at airmass ≤ 2.0. During our selected dates, the Moon is either below the horizon for the first part of the night or remains at low phase and low altitude thereafter. These conditions ensure consistently dark skies throughout each night, minimizing background contamination and allowing all six 8-minute exposures to be taken under optimal conditions.
To constrain the wind acceleration and derive the wind-acceleration parameter β, we plan a two-part observing strategy combining time-resolved monitoring and extended phase coverage. We request observations on **three nights**, each consisting of six consecutive **8-minute** exposures using the HERMES spectrograph in its standard high-resolution mode. These nights are clustered around orbital phase $\phi \sim 0.1$, where wind acceleration is expected to be rapid. This cadence allows us to trace the motion of individual wind clumps over several hours and obtain multiple (a, v) data points per night, where a and v denote radial acceleration and velocity, respectively.
To complement this, we propose single-exposure monitoring on seven additional nights, each with an 8-minute exposure taken near the same hour. These snapshots extend coverage across a full week, enabling us to assess the persistence of spectral substructures and estimate typical clump lifetimes. In favorable cases, clumps that persist across multiple nights may allow us to estimate their 24-hour average acceleration, offering an independent check on the derived β value. This dual strategy balances temporal resolution with phase coverage, while accounting for weather-related risks; the seven-night sampling is flexible, whereas the three high-cadence core nights are prioritized.

Data Analysis: All spectra will be reduced using the HERMES pipeline, which performs wavelength calibration and flat-field correction, yielding normalized line profiles suitable for Doppler analysis. We will focus on the C III, C IV, He I and O V emission lines, which trace different depths of the WR wind. By fitting sub-peaks in each spectrum, we will track clump velocities over time. Averaging over clumps per night reduces short-term noise and yields a set of (a, v) measurements. We aim to reproduce a diagnostic a–v diagram similar to Figure 3 of Lefèvre et al. (2005), which illustrates how different β values shape the acceleration profile.

$$a(v) = v\frac{dv}{dr} = \beta\frac{v^2}{R_*}\left[\left(\frac{v}{v_\infty}\right)^{-\beta/2} - \left(\frac{v}{v_\infty}\right)^{\beta/2}\right]^2, \quad (1)$$

following Lefèvre et al. (2005). Fitting this relation using known v_∞ (Williams et al. 2021) and R_* (Williams 2011) where v_∞ is the terminal wind velocity and R_* is the stellar radius of the Wolf-Rayet star, will enable us to constrain the wind-acceleration parameter β.

6. References and Figures (max. 2 pages)

References:

Dougherty, S. M., Beasley, A. J., Claussen, M. J., Zauderer, B. A., & Bolingbroke, N. J. 2005, The Astrophysical Journal, 623, 447

Eversberg, T., Lepine, S., & Moffat, A. F. J. 1998, Astrophysical Journal, 494, 799

Fahed, R., Moffat, A. F. J., Zorec, J., et al. 2011, Monthly Notices of the Royal Astronomical Society, 418, 2

Gunawan, D. Y. A. S., Van Der Hucht, K. A., Williams, P. M., et al. 2001, Astronomy and Astrophysics, 376, 460

Lefèvre, L., Marchenko, S. V., Lépine, S., et al. 2005, Monthly Notices of the Royal Astronomical Society, 360, 141

Lepine, S. & Moffat, A. F. J. 1999, The Astrophysical Journal, 514, 909

Marchenko, S. V., Moffat, A. F. J., Ballereau, D., et al. 2003, The Astrophysical Journal, 596, 1295

Monnier, J. D., Zhao, M., Pedretti, E., et al. 2011, The Astrophysical Journal, 742, L1

Oskinova, L. M., Hamann, W.-R., & Feldmeier, A. 2007, Astronomy Astrophysics, 476, 1331

Owocki, S. P. & Rybicki, G. B. 1984, Astrophysical Journal, 284, 337

Pollock, A. M. T., Stevens, I. R., Corcoran, M. F., Williams, P. M., et al. 2021, Monthly Notices of the Royal Astronomical Society, 504, 5854

Sundqvist, J. O., Owocki, S. P., Cohen, D. H., Leutenegger, M. A., & Townsend, R. H. D. 2011, Monthly Notices of the Royal Astronomical Society, 420, 1553

Williams, P. 2011, Bulletin de la Société Royale des Sciences de Liège, 80, 595

Williams, P. M., Varricatt, W. P., Chené, A.-N., et al. 2021, Monthly Notices of the Royal Astronomical Society, 503, 643

Zhekov, S. A. 2021, Monthly Notices of the Royal Astronomical Society, 503, 3736

Notes:

We used ChatGPT to correct grammatical mistakes in our writing and used it to refine our writing.

6. References and Figures (max. 2 pages)

Figures:

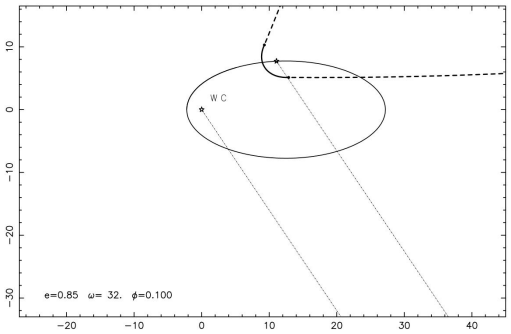

Figure 1. Axes are in astronomical units (AU) with the origin at the WR star. The filled star and open circle mark the WR and O components; black and grey ellipses trace their orbits. Grey dashed lines show the star-centre separation at the observing epoch; the grey wedge is the wind-collision cone (half-opening angle θ = 64°). The bold arrow indicates the downstream flow where clumps migrate. Tracking the clumps' time-dependent radial velocities and accelerations in emission-line profiles then yields a direct fit to the wind-acceleration index . Orbital parameters adopted: e = 0.88, i = 122°, ϕ = 0.100. (Gunawan et al. 2001).

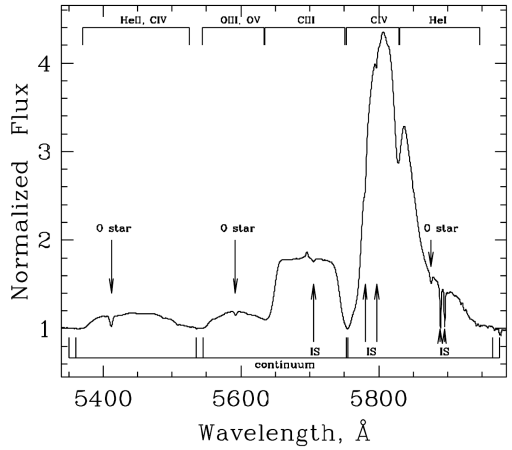

Figure 2. Mean spectrum of WR 140 based on constant spectra. Bars at the top indicate the ranges of various WR emission lines. O-star photospheric absorption lines along with interstellar features. This is a published spectrum from the work of Marchenko et al. (2003)

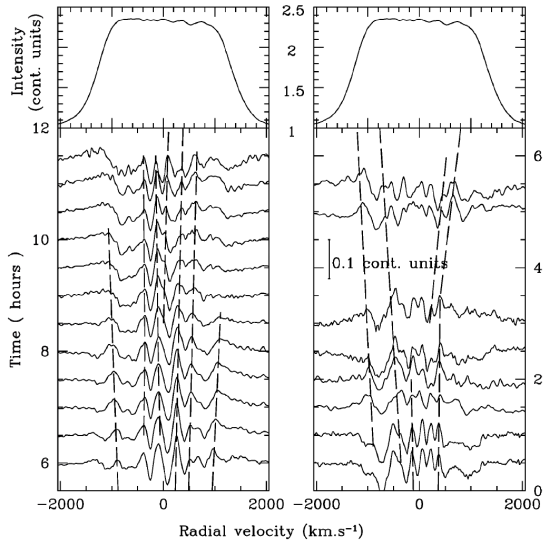

Figure 3. Residual line-profile variations of C III 5696 (left) and C IV 5808 (right) during the post-periastron observations of WR 137 (Lefèvre et al. 2005). In each panel the top curve is the mean emission profile and below it the residuals (each offset vertically) reveal transient "bumps" from individual wind clumps. The motion of these bumps in radial-velocity space tracks the clump velocity evolution, and the slope of the dashed guide-lines corresponds to the local acceleration hence to the wind-acceleration parameter β.

7. Justification of requested observing time and lunar phase

Lunar Phase Justification: No constraints

Time Justification: (including seeing overhead) We request a total of 200 minutes to carry out a two-part observing strategy aimed at constraining the wind acceleration and exponent in WR 140. Our goal is to achieve a signal-to-noise ratio (S/N) of approximately 200 at 550nm, which is required in orevious studies (Lefèvre et al. (2005)) for detecting subtle radial velocity shifts and resolving fine spectral substructures associated with individual wind clumps. Using the Mercator–HERMES Exposure Time Calculator (HRF mode, dark sky, 0.8 seeing, 0.1% slit loss,Vmag = 6.85, spectral type = O, E(B–V) = 0.00, Ron= 3.5, airmass = 2.0), we find that an 8-minute exposure yields S/N = 200 per pixel even at an elevation of 30° (airmass = 2), which defines the lowest elevation we expect during observations. Therefore, we adopt a uniform 8-minute exposure time across all nights to ensure consistent S/N and data quality. On three consecutive nights, we request six 8-minute exposures per night to achieve the temporal resolution needed to measure clump acceleration over a few hours. On seven additional nights, we request one 8-minute exposure per night to sample the same orbital phase region over a full week. This cadence allows us to track short-term velocity changes and assess clump lifetimes, while ensuring consistent S/N = 200 across all observations.

Calibration Request: Standard Calibration

8. List of MERCATOR targets proposed in this programme

Run	Name	R.A. (J2000)	Dec. (J2000)	V (mag)	ToT (hr)
A	WR 140	20 20 28	43 51 16	6.85	3.3

MERCATOR Target Notes: Not Applicable

MERCATOR Set-up: HERMES HRF mode